

Measurement of the Sheath Potential with Secondary Electron Emission: Progress toward a Laser-Induced Fluorescence Technique for Low-Density Xenon Plasmas

IEPC-2013-459

*Presented at the 33rd International Electric Propulsion Conference,
The George Washington University • Washington, D.C. • USA
October 6 – 10, 2013*

Alexander C. Englesbe¹, Kapil U. Sawlani² and John E. Foster³
University of Michigan, Ann Arbor, Michigan, 48109, USA

Abstract: Secondary electron emission (SEE) at bounding surfaces in plasmas is known to alter the sheath potential at the boundary, typically reducing its magnitude. Such changes affect energy transport to the walls and also presumably influence the bulk plasma electron energy distribution function. In crossed-field devices such as Hall thrusters, SEE in combination with other factors has also been shown to enhance cross-field electron transport. In order to understand the degree to which SEE modifies the sheath potential, and in turn bulk electron energetics, we measure the sheath potential in the presence of a secondary electron flux leaving a solid surface. In preparation for laser-induced fluorescence (LIF) sheath measurements aimed at mapping the potential distribution in the sheath, a rough characterization of the sheath size over a range of plasma densities is carried out first using an emissive probe. Ultimately, the goal of this work is to fully resolve the sheath structure using LIF by operating the plasma source under thick sheath conditions. Also, some obstacles to using LIF to spatially resolve the sheath, such as signal suppression associated with intense filament light emission, are addressed.

Nomenclature

k_B	= Boltzmann constant
r_{pr}	= Probe radius
T_e	= Electron temperature
V_p	= Plasma potential

I. Introduction

EMISSION of secondary electrons from the walls of the discharge channel in Hall-effect thrusters is believed to have a significant effect on thruster efficiency and lifetime, since it has been shown to play a major role in the physics of the Hall thruster discharge. This is in part due to the ability of secondary electron emission (SEE) to generally lower the electron temperature in the thruster plasma^{1,2}. SEE also contributes to anomalous cross-field electron transport and near-wall conductivity³. Simulations indicate that the former arises due to an instability induced by SEE in the sheath at the discharge channel wall⁴. Overall, the nature of the plasma-surface interaction is governed by the electron energy distribution function⁵, whose high-energy tail is depleted by the interaction with the

¹ Graduate Student Research Assistant, Department of Nuclear Engineering and Radiological Sciences, aengles@umich.edu.

² Graduate Student Research Assistant, Department of Nuclear Engineering and Radiological Sciences, sawlanik@umich.edu.

³ Associate Professor, Department of Nuclear Engineering and Radiological Sciences, jefoster@umich.edu

walls and the ejection of cold secondary electrons into the plasma⁶. The overall effect of secondary electrons on crossed-field plasmas such as that in a Hall thruster is not fully understood, and control over their effects on Hall thruster operation is desirable.

Secondary electrons originate in the wall material and must traverse the sheath in order to enter the main discharge. The sheath potential drop, which is expected to be of the order of $k_B T_e$ facilitates thermalization of the electrons if they enter the discharge, although a significant fraction of secondary electrons become trapped near the wall in a Hall thruster⁷. These circumstances lead to modification of the sheath potential structure. Indeed, secondary electron emission from a bounding surface in a plasma even in the absence of electron trapping causes reduction of the sheath potential drop⁸. Since it is self-consistent with transport across the plasma boundary, the sheath potential is a direct indicator of the entry of secondary electrons into the Hall thruster discharge.

The study endeavors to understand the conditions that determine secondary electron yield in a plasma whose properties, while quite different from those of a Hall thruster, are chosen so that secondary electron effects may be easily observed. Experiments to spatially resolve the sheath potential structure are performed in order to establish a correlation between the shape of the sheath potential and the plasma conditions, including secondary electron emission. This paper discusses the results of emissive probe measurement of the sheath potential, as well as plans for using laser-induced fluorescence (LIF) to achieve a finessed measurement. The ultimate goal of the project is to develop a LIF technique which can be used to accurately measure the sheath potential under the plasma conditions of interest.

II. Experimental Setup

While magnetic field effects are an integral part of Hall thruster physics, this experiment dispenses with the magnetic fields for the sake of achieving the simplest possible relationship between the plasma properties and the bounding sheath. That is, electron transport need not be considered in the context of components which are parallel and transverse to the field lines, and there are no field lines which terminate on the target surface. Furthermore, while typical Hall thrusters operate at plasma densities of 10^{10} - 10^{12} cm⁻³, the plasma in these experiments is of a much lower density (10^7 - 10^8 cm⁻³) so as to maximize the sheath thickness and afford the measurements the best possible spatial resolution.

A. Plasma Source

A multipole ring-cusp discharge chamber shown in Fig. 1 confines a xenon plasma. It consists of a cylindrical shell anode lined with three rows of permanent cobalt-samarium magnets. The source is hot filament-driven. The source is terminated at its most downstream end with a grid electrode. Two viewing windows near the grid provide optical access for laser-based diagnostics. In order to generate and sustain the discharge, it is necessary to bias the anode to approximately +40 V.

A small volume in the source interior near the grid surface is approximately field-free. The target material whose sheath is measured is mounted to the grid in this field-free region. The target is a 5 cm x 10 cm section of aluminum plate. The magnetic field strength at the target surface is less than 10 G. The field strength increases to about 30 G at a 3 cm distance from the target surface.

With the planned LIF experiments in mind, it is important to consider factors which would reduce the fluorescence signal-to-noise ratio. Because the radiant emissions of the filament are very bright across the visible and near-infrared regime, spectral overlap between these emissions and the fluorescence signal is anticipated to have deleterious effects on the quality of the measurement. A rudimentary way to reduce the relative brightness of the filament is to partially block its emissions with a solid barrier, as in Fig. 2. The plasma source may be outfitted with this barrier, or baffle which casts a shadow on the grid-side of the source, preventing direct line-of-sight between the

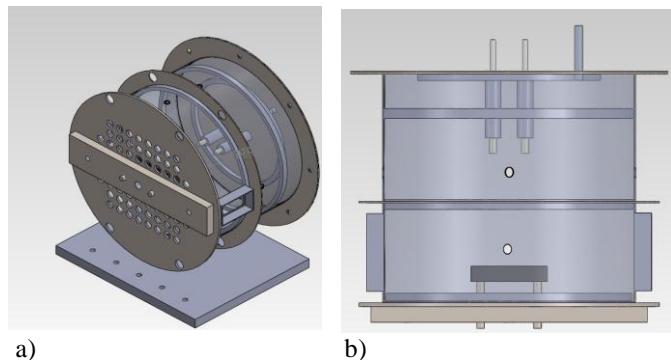


Figure 1. a) An isometric view of the multipole ring-cusp plasma source. b) A view from the top showing the filament holders (top of the figure) and the target (bottom of the figure).

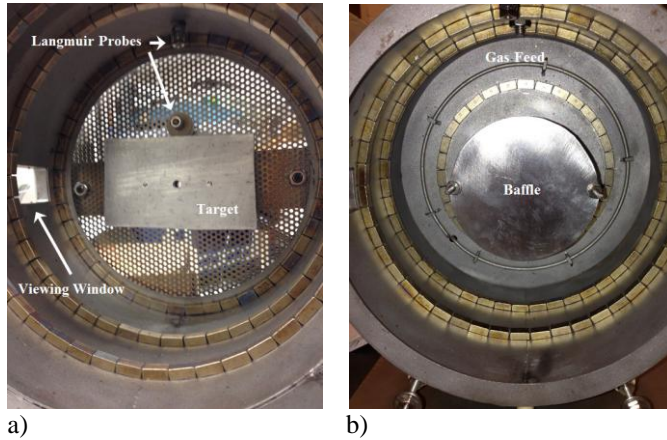


Figure 2. a) Internal view of the plasma source showing the aluminum target with a through-hole for emissive probe access. b) An internal view from the opposite side with the baffle in place covering the cathode filament.

0.0025 mm. The motion controller translates the probe through the sheath along the axial coordinate of the plasma source, and measurements of the local plasma potential are made at 0.5 mm, 1 mm and 2 mm intervals. The 0.5 mm steps are needed to resolve the sheath, while the 1 and 2 mm steps are sufficient to observe the pre-sheath. The diameter of the tungsten wire is 0.1mm. The tungsten leads are inserted into capillary alumina tubing in order to improve the spatial resolution of the probe. For this probe design, the resolution is a few times the wire diameter. The plasma potential is determined using the floating point method in the limit of large emission.

An Ocean Optics USB2009 spectrometer is fiber coupled to one of the viewing windows in order to measure emissions from the filament and the plasma. The resolution of the spectrometer is about 1 nm, and therefore is useful for a relatively coarse spectral characterization the emissions.

C. Laser-Induced Fluorescence

The LIF level scheme for Xe^+ which will be employed in the sheath potential measurements follows Severn and colleagues⁹. A laser wavelength of 680.6 nm excites the $5d^4F_{7/2} - 6p^4D^0_{5/2}$ transition, which decays to the $6s^4P_{3/2}$ level with a fluorescence wavelength of 492.1 nm. The fluorescence will be stimulated by a Sacher Lasertechnik Lynx-100 tunable diode laser whose output power is 25mW at 670 nm. The laser beam will pass through a mechanical chopper so that a lock-in amplifier may be used to recover the LIF signal from the noisy background created by the plasma and filament. By focusing the detector on different locations along the beam path in the vicinity of the target, the local ion velocity distribution may be calculated based on the broadening of the fluorescence lineshape. These measurements are quite similar to those carried out by Lee and colleagues¹⁰.

III. Results

A. Source Characterization

In order to spatially resolve the sheath structure at the target using an emissive probe, the sheath at the target must be made as large as possible. This is most easily accomplished by reducing the plasma density, which depends on the discharge voltage, filament current, and gas pressure. Some of the plasma properties measured in a parameter space search for conditions resulting in thick sheaths are summarized in Figs. 4 and 5. Plasma properties are calculated from Langmuir probe traces. The judgment of whether or not the sheath is thick enough to be suitable for the spatially-resolved emissive probe measurements is made on the basis of the Debye length, which is calculated using the measured electron temperature and the plasma density inferred from the ion saturation current.

The effects of the grid and discharge voltages on the sheath thicknesses are illustrated in Figs. 4d and 5d. Since increasing the discharge voltage tends to also increase the amount of ionization that occurs, lower plasma densities

filament and the fluorescence signal detector. The baffle may also be used to moderate the energy of the beam electrons leaving the filament.

B. Probes and Diagnostics

There are two Langmuir probes affixed to the inside of the source, shown in Fig. 2a. Since these experiments target low plasma densities, the probes, which have identical dimensions, are large ($r_{pr} = 4.38$ mm rod) in order to ensure the collection of appreciable saturation current.

An emissive probe, shown in Fig. 3 is mounted to a precision motion controller, whose step resolution is



Figure 3. A translatable emissive probe. The alumina stem is coated to reduce secondary electron emission from the probe itself.

can be achieved by minimizing the discharge voltage at which the plasma remains stable. For the same reason, lower densities can be reached by reducing the filament current. Since the grid is positively biased, it serves as a large collection surface for electrons. Increasing the grid voltage also increases the loss rate of electrons, leading to a lower density in the vicinity of the grid, and therefore the target. Under these conditions, ion densities of about $5 \times 10^7 \text{ cm}^{-3}$ can be achieved, and ion Debye lengths can reach about 2 mm.

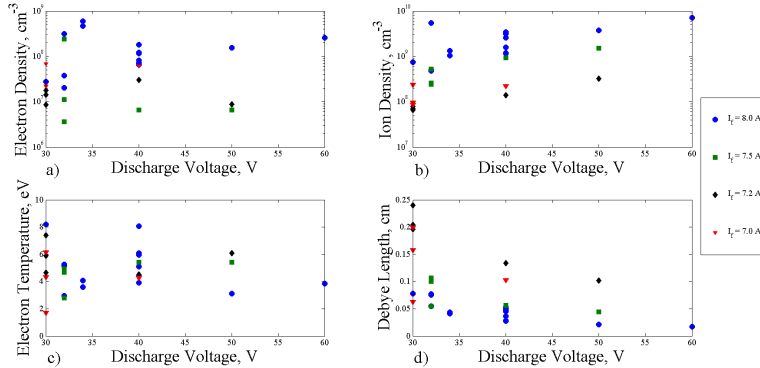


Figure 4. Plasma properties as a function of the discharge voltage: a) electron density, b) ion density, c) electron temperature and d) Debye length.

data are obtained while operating the source at a discharge voltage of 35 V, a discharge current of 183 mA, a chamber pressure of 5.2×10^{-5} Torr, a xenon flow rate of 1.2 sccm, while driving 7.0A through the cathode filament. The plasma density is $7 \times 10^8 \text{ cm}^{-3}$. Judging by the shape of the potential distribution, the sheath and pre-sheath have been resolved. The pre-sheath electric field appears to be about 4 Vcm^{-1} .

C. Obstacles for LIF – Filament Brightness Reduction

So far, modest reduction of the filament brightness has been achieved by covering the filament with a metal baffle, which blocks direct line-of-sight between the filament and the viewing windows. Figure 7 shows example spectra collected with and without the baffle in place at the same filament current. There is some reduction in the brightness of the filament as seen by the detector. Figure 7 illustrates the problem of spectral overlap between the filament emissions and the LIF fluorescence

signal, as the filament emissions at the LIF fluorescence wavelength are about half as bright as the maximum spectral brightness of the filament. Even if a bandpass wavelength filter is used to discriminate light which can enter the detector, there will be a large contribution from the filament upon which the LIF signal will be superimposed. This will cause a reduction in the signal-to-noise ratio. Furthermore, in order to create the thick sheaths, the plasma density must be quite low, so the number of Xe^+ ions providing the fluorescence will be relatively small, and the LIF signal will be weak. Indeed, examination of the spectra recorded during the experiments reveals that the plasma luminosity is negligible relative to that of the filament at the low densities needed for proper sheath thickness and spatial resolution of the sheath potential measurements.

Attempts to diminish the filament brightness further will involve re-designing the baffle to block more of the scattered filament emissions. Also, reducing the filament temperature will cause the center of the grey body spectra in Figure 7 to shift toward the infrared, and away from the fluorescence wavelength. It is possible that if the reduction needed to achieve minimal filament emission at 492.1 nm is small enough, the resulting decrease in thermionic emission from the filament will not prevent the formation of a stable discharge.

B. Emissive Probe Measurement of the Sheath Potential

Figure 6 shows the local plasma potential measured by the emissive probe as a function of distance from the target surface. The emissive probe

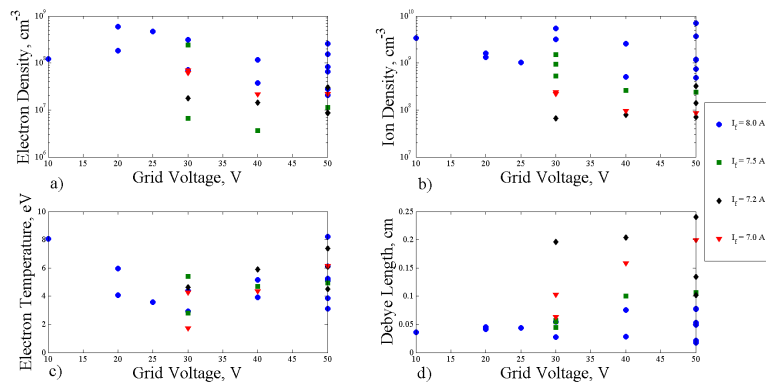


Figure 5. Plasma properties as a function of the grid voltage: a) electron density, b) ion density, c) electron temperature and d) Debye length.

IV. Concluding Remarks

In this work, the discharge operating regimes for thick sheaths are mapped out and documented. These conditions will be probed using LIF to quantify sheath shape at a target irradiated with an electron beam. Preliminary emissive probe measurements confirm thick sheath profiles anticipated from Debye length calculations. Additionally, the use of a baffle to reduce scattered light from the filament is demonstrated. Modest reductions are observed, and a more aggressive approach appears to be necessary to prevent the filament light from washing out the LIF signal.

Acknowledgments

The author thanks the NASA Michigan Space Grant Consortium for support through its Graduate Fellowship Program. This work is supported by the Air Force Office for Scientific Research through Grant No. FA9550-09-1-0695.

References

- ¹Raitses, Y., Smirnov, A., Staack, D., and Fisch, N.J. "Measurements of secondary electron emission effects in the Hall thruster discharge," *Physics of Plasmas*, Vol. 13, 014502, Jan. 2006.
- ²Keidar, M., Boyd, I.D. and Beilis, I.I. "Plasma flow and plasma-wall transition in Hall thruster channel", *Physics of Plasmas*, Vol. 8, No. 12, 2001, pp. 5315-5322.
- ³Raitses, Y., Kaganovich, I.D., Khrabrov, A., Sydorenko, D. Fisch, N.J., and Smolyakov, A. "Effect of Secondary Electron Emission on Electron Cross-Field Current in $E \times B$ Discharges," *IEEE Transactions on Plasma Science*, Vol. 39, No. 4, 2011, pp. 995-1006.
- ⁴Taccogna, F., Longo, S., Capitelli, M. and Schneider. "Anomalous transport induced by sheath instability in Hall effect thrusters," *Applied Physics Letters*, Vol. 94, 251502, June 2009.
- ⁵Sydorenko, D., Smolyakov, A., Kaganovich, I., and Raitses, Y. "Modification of Electron Velocity Distribution in Bounded Plasmas by Secondary Electron Emission," *IEEE Transactions on Plasma Science*, Vol. 34, No. 3, 2006, pp. 815-824.
- ⁶Ahedo, E., de Pablo, V., and Martínez-Sánchez, M. "Effects of partial thermalization and secondary emission on the electron distribution function in Hall thrusters," *29th International Electric Propulsion Conference*, 2005, pp. 1-11.
- ⁷Ahedo, E., and Parra, F.I. "Partial trapping of secondary-electron emission in a Hall thruster plasma," *Physics of Plasmas*, Vol. 12, 073503, June 2005.
- ⁸Hobbs, G.D. and Wesson, J.A. "Heat flow through a Langmuir sheath in the presence of electron emission," *Plasma Physics*, Vol. 9, 1966, pp. 85-87.
- ⁹Severn, G., Lee, D., and Hershkowitz, N. "Xenon ion laser-induced fluorescence using a visible tunable diode laser near 680 nm," *Review of Scientific Instruments*, Vol 78, No. 11, 116015, 2007.
- ¹⁰Lee, D., Hershkowitz, N., and Severn, G. "Measurements of Ar^+ and Xe^+ velocities near the sheath boundary of Ar-Xe plasma using two diode lasers," *Applied Physics Letters*, Vol. 91, No. 4, 041505, 2007.

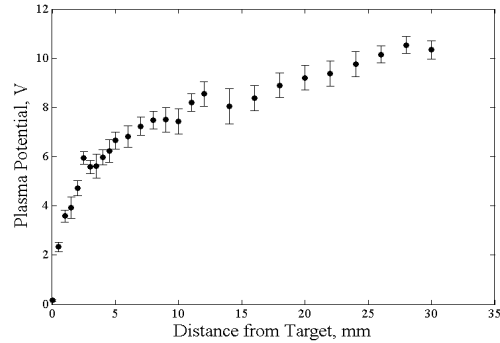


Figure 6. Local plasma potential as a function of distance from the surface of the target.

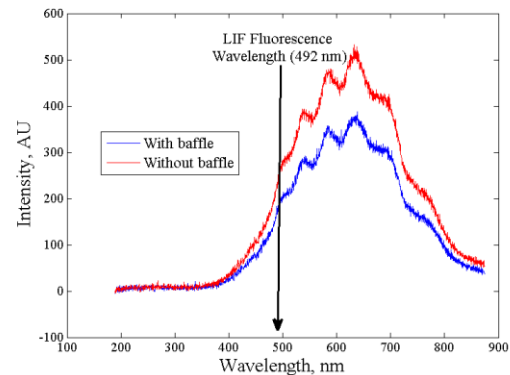


Figure 7. Comparison of radiant the spectrum of the cathode filament in the plasma source with and without the baffle partially blocking the emissions.